Journal of Hazardous Materials 183 (2010) 138–144

Contents lists available at ScienceDirect

Journal of Hazardous Materials

journal homepage: www.elsevier.com/locate/jhazmat

Using of multi-walled carbon nanotubes electrode for adsorptive stripping voltammetric determination of ultratrace levels of RDX explosive in the environmental samples

Behzad Rezaei*, Sajjad Damiri

Department of Chemistry, Isfahan University of Technology, Isfahan 84156-83111, Iran

ARTICLE INFO

Article history:
Received 30 January 2010
Received in revised form 1 June 2010
Accepted 30 June 2010
Available online 7 July 2010

Keywords:
Multi-walled carbon nanotube
RDX
Explosive
Adsorptive stripping voltammetry
Electrochemical impedance spectroscopy

ABSTRACT

A study of the electrochemical behavior and determination of RDX, a high explosive, is described on a multi-walled carbon nanotubes (MWCNTs) modified glassy carbon electrode (GCE) using adsorptive stripping voltammetry and electrochemical impedance spectroscopy (EIS) techniques. The results indicated that MWCNTs electrode remarkably enhances the sensitivity of the voltammetric method and provides measurements of this explosive down to the sub-mg/l level in a wide pH range. The operational parameters were optimized and a sensitive, simple and time-saving cyclic voltammetric procedure was developed for the analysis of RDX in ground and tap water samples. Under optimized conditions, the reduction peak have two linear dynamic ranges of 0.6–20.0 and 8.0–200.0 mM with a detection limit of 25.0 nM and a precision of <4% (RSD for 8 analysis).

1. Introduction

The explosives and related compounds detection have been more considering for national security and environmental applications [1,2]. Pollution of both soils and ground waters by Research Department explosive (RDX), high melting point explosive (HMX) and other nitroaromatic and nitramine explosive compounds is a significant worldwide problem [3–6]. The main sources of these toxic explosive contaminants are manufacturing, testing and disposal of explosives by defense establishments. These compounds are mutagenic, toxic and have the tendency to persist in the environment [7–9]. RDX and HMX are major ingredients in nearly every ammunition formulation and are the secondary explosives used in the greatest quantities. RDX is toxic to a wide range of organisms including terrestrial, soil dwelling and aquatic organisms due to its cytotoxicity, genotoxicity, neurotoxicity or possible carcinogenicity. Practically, explosive contaminants in soil may undergo metabolic transformation, photo catalytic degradation and biodegradation by various processes such as, oxidation, dehydrogenation, reduction, hydrolysis and exchange reactions [10–12].

Up to now, various analytical methods have been reported for the determination of RDX based on the spectroscopy [13,14], capillary electrophoresis [15,16], gas chromatography [17–20], high performance liquid chromatography (HPLC) [21–24], ion mobility spectrometry [25] and voltammetry [26,27] techniques. Electrochemical sensors offer great prospects for addressing the growing needs for field detection of various explosives. The advantages of electrochemical techniques for on-site measurements of explosives are included, high sensitivity and selectivity, a wide linear range, minimal space and power requirements, and low cost instrumentation. Most of reports, on the electroanalytical determination of the energetic materials, have been focused on the determination of trinitrotoluene (TNT) as a common explosive material. The performance of voltammetric procedures is strongly influenced by the working electrode materials and constructions. A range of techniques have found application for reductive (cathodic) measurements of nitroaromatic and nitramine explosive compounds, including mesoporous SiO_2-modified electrode [28], voltammetry on microfluidic chip platforms [29], gold electrode modified with self-assembled monolayer [30], electrochemical immunoassay based on functionalized silica nanoparticle labels [31], hanging drop mercury electrode [32], carbon-fiber electrode [33], screen printed electrode [34], carbon nanotubes [35,36] and various forms of carbon (fiber, diamond, glassy carbon), or gold/amalgam electrodes [37,38].

Carbon nanotubes (CNTs) continue to receive remarkable attention in electrochemistry. The modification of electrode substrates with multi-walled carbon nanotubes (MWCNTs) using in analytical sensing have been developed to achieved, low detection limits, high sensitivities, reduction of over-potentials and resistance to

* Corresponding author. Tel.: +98 311 3912351; fax: +98 311 3912350.
E-mail address: rezaei@cc.iut.ac.ir (B. Rezaei).

0304-3894/$ – see front matter © 2010 Elsevier B.V. All rights reserved.
doi:10.1016/j.jhazmat.2010.06.127

surface fouling [39,40]. CNTs have been introduced as electrocatalysts and their modified electrodes have been reported to give super performance in the studies of some biological and pharmaceutical species [41–43]. Compton and Banks' group has demonstrated for most electroactive species, via the comparison of MWCNT-modified electrodes with edge plane pyrolytic graphite electrodes, that usually the electroactive sites of the MWCNTs are edge plane-like sites/defects which can occur at the ends of the nanotubes or along the nanotube where tube compartments terminate [44–46].

The objective of the current work is to develop a suitable and sensitive method for the determination of RDX, based on the unusual properties of CNTs such as strong adsorptive ability, huge specific area, subtle electronic properties as well as excellent electrocatalytic activity. Thus, the electrochemical behavior of RDX on the multi-wall carbon nanotube-coated glassy carbon electrode (GCE) was investigated by voltammetry and electrochemical impedance spectroscopy techniques to better estimation of interaction between RDX and nanotubes. The results showed that MWCNTs strongly enhanced the electron transfer rate of RDX reduction and its determination sensitivity was significantly improved. At the MWCNTs coated GCE, the remarkable peak current enhancement and shift of peak potential occurred for RDX reduction in compare of bare GCE. Consequently, an ultrasensitive adsorptive stripping voltammetric method based on the carbon nanotube-modified electrode was developed for the determination of ultratrace levels of RDX in the environmental samples. This proposed method provides some advantages such as high sensitivity, rapid response, low cost and simplicity.

2. Experimental

2.1. Apparatus and reagent

Electrochemical measurements were carried out in a conventional three-electrode cell, powered by an electrochemical system comprising the Autolab system with PGSTAT 12 and FRA2 boards (Eco Chemie B. V., Utrecht, Netherlands). The system was run on a PC using GPES and FRA 4.9 software. For impedance measurements, a frequency range of 100 kHz to 10 MHz was employed. Applied amplitude of AC voltage and equilibrium time was 5 mV and 20 min, respectively. The MWCNTs modified GCE, a graphite electrode and a saturated Ag/AgCl reference electrode was employed as a working, auxiliary and reference electrode, respectively.

The MWCNTs were bought from Iran's Research Institute of Petroleum Industry and synthesized by chemical vapor deposition (CVD) with a diameter of 8–15 nm, a length 50 μM and the purity of 95%. The modified electrodes with carbon nanotube layers were characterized by scanning electron microscopy (SEM). RDX and other explosive materials with the purity of >99.0% were purchased from Iranian defense industries. The RDX stock solution, 0.002 M was freshly prepared in methanol–water solution (1:1, v:v).

Universal buffer (boric acid, phosphoric acid, acetic acid and sodium hydroxide, 0.10 M) solutions with different pH values were used for the study of influence of the electrolyte pH on the signals. All aqueous solutions were prepared and diluted with deionized water (resistivity not less than 18.0 MΩ at 25 °C).

2.2. Preparation of MWCNT suspension and modified GCE

To eliminate metal oxide impurities within the nanotubes, multi-walled carbon nanotubes were refluxed in the presence of 2.0 M HNO_3 for 15 h, then washed with twice-distilled water and dried at room temperature. 0.010 g of purified MWCNTs was dispersed in 10.0 ml dimethylformamide (DMF) by using ultrasonic agitation to obtain a relative stable suspension. The GCE was carefully polished using 0.05 μm alumina slurry on a polishing cloth, and then washed ultrasonically in methanol and water, respectively. The cleaned GCE was coated by casting 300.0 μl of the black suspension of MWCNTs and dried in an oven at 60 °C. The microscopic areas of the MWCNT-modified GCE and the bare GCE were obtained by cyclic voltammetry (CV) using 1.0 mM $K_3Fe(CN)_6$ as a probe at different scan rates. For a reversible process, the Randles–Sevcik formula has been used:

$$I_{pa} = 2.69 \times 10^5 (\mathrm{A\,s\,mol^{-1}V^{-1/2}}) n^{3/2} A C_O D_R^{1/2} \nu^{1/2} \quad (1)$$

where I_{pa} refers to the anodic peak current (A), n is the electron transfer number, A is the surface area of the electrode (cm^2), D_R is diffusion coefficient ($cm^2\,s^{-1}$), C_O is the concentration ($mol\,cm^{-3}$) of $K_3Fe(CN)_6$, and ν is the scan rate ($V\,s^{-1}$). For 1.0 mM $K_3Fe(CN)_6$ in the 0.10 M KCl electrolyte: $n = 1$ and $D_R = 7.6 \times 10^{-6}\,cm^2\,s^{-1}$, then from the slope of the I_{pa}–$\nu^{1/2}$ relation, the microscopic areas can be calculated. On the bare GCE, the electrode surface area was 0.0314 cm^2 and for MWCNT-modified GCE the microscopic area was found 2.9–3.0 times greater.

2.3. Analytical procedure

4.0 ml of ground water or tap water samples were spiked with RDX solution and were diluted to 10.0 ml with 0.10 M buffer solution with pH 7.0. Then, these solutions were transferred to the electrochemical cell and the determination of RDX was carried out by CV method. In these studies, above solutions, in the electrochemical cell, were de-oxygenated and stirred with nitrogen gas at the desired accumulation potential for a given period of time. Then, the solution was allowed to rest for 15 s, and the electrode potential was scanned between −0.30 and −1.00 V. After each electrochemical measurement, the electrode was slightly rinsed with methanol and water to renew its surface. In all cases, the standard addition method was used for the determination of analyte in the real samples.

3. Results and discussion

3.1. Characterization of MWCNT-modified electrode

The dispersing state of the MWCNTs was examined by scanning electron microscopy. SEM micrographs showed that most of MWCNTs were well dispersed in DMF and no longer entwined together.

Electrochemical impedance spectroscopy (EIS) can also provide some information about impedance changes of the electrode surface or its electron transfer ability during the modification process. The experiments were performed for 1.0 mM $K_3Fe(CN)_6$ in 10.0 mM KCl electrolyte, and EIS data were recorded at the dc-offset potential +0.30 V and frequency range of 100 kHz to 10 MHz. A typical Nyquist plot for this system consists of a semicircle portion observed at higher frequency range corresponding to the electron transfer-limited process and a linear part at lower frequencies representing the diffusion limited process. The EIS data were approximated using FRA 4.9 software and complex nonlinear least square (CNLS) approximation method, from which electron transfer kinetics as charge transfer resistance (R_{ct}), solution resistance (R_s), double-layer capacitance (C_{dl}) or constant phase element (CPE) and mass transfer element W (Warburg impedance) were extracted. The EIS data obtained at the GCE was fitted to the Randles circuit: $R_s(C[R_{ct}W])$, but for MWCNTs electrode the modified Randles' model in which C_{dl} was replaced by frequency-dependent constant phase element was used to explain experimental data. By using this method, the electron transfer resistance R_{ct}, on the bare GC and MWCNTs electrodes obtained 46.0 and 12.6 Ω cm^2, respectively. Thus, the charge transfer resistance at the nanotube-modified electrode is significantly lower than of its resistance at the

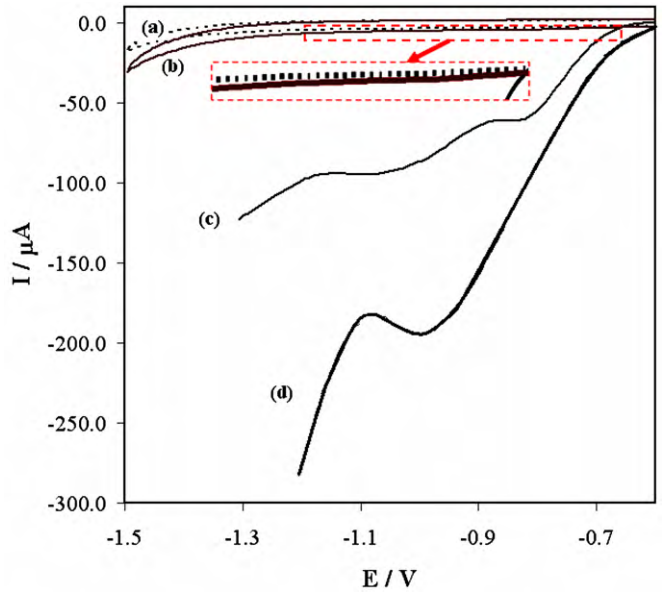

Fig. 1. Cyclic voltammograms of RDX at the GC electrode; (A) background, (B) at the presence of 60 μM RDX and background subtracted voltammograms for 60 μM RDX on the MWCNTs electrode in the pH 7.0 (C) and pH 2.0 (D). Other conditions; scan rate of 50 mV s^{-1}, accumulation potential of −0.1 V and accumulation time of 7.0 min.

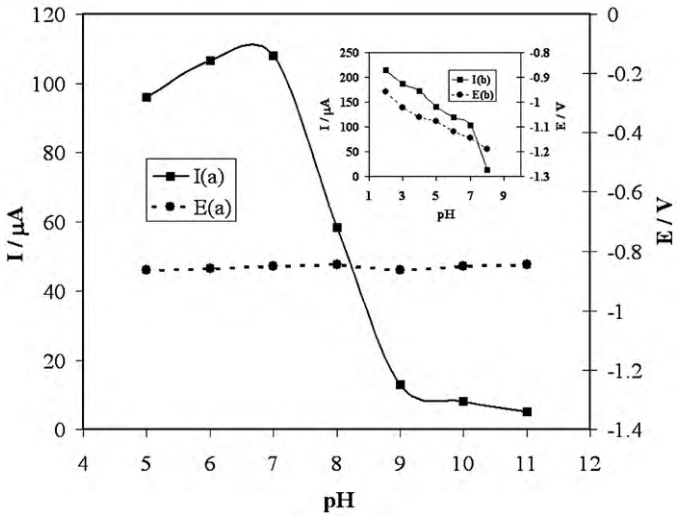

Fig. 2. Effect of pH on the peak current and potential at the modified electrode of first reduction reaction. Other conditions, scan rate of 50 mV s^{-1}, 60 μM RDX, accumulation potential of −0.1 V and accumulation time of 7.0 min. Inset shows the related data for the second peak.

GCE, which means it has stronger hindrance to the electron transfer of hexacyanoferrate.

3.2. Electrochemical behavior of RDX on GCE and MWCNT-modified electrode

The voltammetric responses of 60 μM RDX on the bare and MWCNTs modified electrode was studied over the pH interval 2.0 to 11.0 by using CV. According to Fig. 1, it is observed that the cathodic reduction of RDX on the bare glassy carbon electrode shows an nil defined peak attributed to the reduction of nitro group. But under the similar conditions, RDX yields two well-defined and pH dependent reduction peaks on the MWCNTs modified electrode, and the reduction peak current significantly increases in compare of bare GCE. This increasing in the peak current and declining of reduction potential are clear evidences of the catalytic effects of the MWCNTs toward the reduction of RDX. In the acidic solutions (pH < 5), the reduction reactions occur rapidly and the mentioned peaks mix together.

3.3. Effect of solution pH on the peak potentials and peak currents

The reduction behavior of RDX closely depends on the pH of solution. This explosive can be hydrolyzed in the basic solution and produce some ions such as NO_2^- (nitrite), $HCOO^-$ (formate) and other related cyclic nitramines [47,48]. Experimental results for 60 μM RDX in 0.10 M buffer solution in the different pHs from 2.0 to 11.0 have been shown in Fig. 2. It can be seen that the direct reduction of RDX presents the higher voltammetric signal in the lower pHs. Obviously investigated that the nitro group reduction of this compounds occurs in the acidic and neutral solutions, whereas the decomposition of RDX to some anions in higher pH values prevents to its suitable interaction with working electrode, thus in these mediums, decrease the reduction currents and difference potentials between two reduction peaks (Fig. 2). Potential of the first peak (peak "a"), which is appeared in pH range of 5.0 to 11.0, has not significant changes. It's indicating that hydrogen ions did not participate in this reduction reaction. Also, shifting of the second peak potential (peak "b") towards the negative direction at higher pHs implies that the reduction process takes up with hydrogen ions. Sketch of peak potentials verses pH value for the second peak was found to be linear over the pH range 2.0–8.0, which is similar to other reports [26], with a slope of -35.8 ± 1.3 mV pH^{-1}. Resulted slope, in this reduction reaction, suggests that the contribution of the electrons is nearly two times higher than H^+ protons.

In this study, we used the first reduction step (peak "a") on a MWCNTs modified electrode as an analytical signal for the determination of RDX in the ground and tap water samples and optimized the various parameters that can affect on the sensitivity of method. These experiments were employed at pH 7.0.

3.4. Effect of scan rate on the peak currents and peak potentials

The effects of scan rate over the range of 10.0–120.0 mV s^{-1} on the first peak current and potential were investigated at the MWCNTs modified electrode by CV for 60 μM RDX at the pH 7.0 (0.10 M universal buffer). The cathodic peak current linearly increased with the square root of scan rate, and the following equation obtained: $I(\mu A) = 626.34\ (\pm 13.61) \times \upsilon^{1/2}\ (V\,s^{-1}) - 60.77\ (\pm 6.73)$, $R^2 = 0.9934$. It's indicating a diffusion controlled reduction process occurring at the modified electrode. Therefore scan rate of 100 mV s^{-1} was selected as the optimum for determination of RDX. The linear relationship between the peak potential (E) and logarithmic scan rate (υ) of an irreversible process obeys the following equation [49]:

$$E(V) = E'_O(V) - \frac{RT}{\alpha nF}(V)\left[0.780 + \ln\left[\left(\frac{D_O^{1/2}}{k_0}\right)/(s^{1/2})\right] + \ln\left[\left(\frac{\alpha nF\upsilon}{RT}\right)^{1/2}/(s^{-1/2})\right]\right] \quad (2)$$

where E'_O is the formal potential, α represents transfer coefficient, n is number of electrons involved in an electrode reaction, F indicates Faraday constant, D_O represents diffusion coefficient, k_0 is standard heterogeneous rate constant, R is gas constant and T is absolute temperature (300 K). The relationship between the peak potential and the scan rate (between 40 and 140 mV s^{-1}) demonstrated by the equation: $E(V) = -0.13\ (\pm 0.031) \times \ln[\upsilon(V\,s^{-1})] - 1.13$

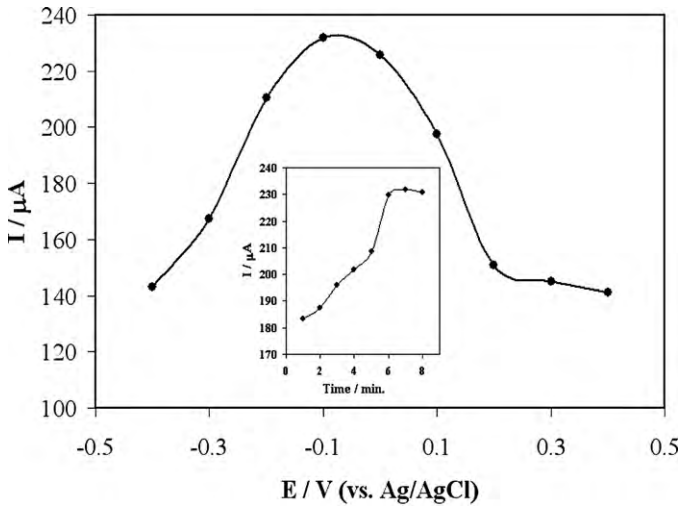

Fig. 3. Effects of accumulation potential on the reduction peak current of 60 μM RDX at the scan rate of 100 mV s^{-1} and pH 7.0. Inset shows effect of accumulation time on the signal.

(±0.051), R^2 = 0.9936, $RT/2n\alpha F$ = 0.13 V and the $n\alpha$ value was calculated to be 0.098 (for peak "a"). Also, the slopes of tafel plots (E vs. log(I_p)) in the low scan rates (5–20 mV s^{-1}) confirm this value of $n\alpha$. From the mentioned results, the two-step reduction reactions can be attributed to the formation of nitroso or hydroxyl amine groups. In the first step, each nitro group can take one electron (without contribution of protons), and subsequently is converted to hydroxyl amine and amine groups at more negative potentials.

3.5. Effects of accumulation potential and time

The reduction peak currents of 60 μM RDX were measured by CV method at different potential from −0.4 to +0.4 V in pH 7.0 and accumulation time 7.0 min. According to Fig. 3, it is observed that the adsorptive stripping response of RDX increases rapidly upon decreasing the accumulation potential, then it rapidly diminishes at the points which are near to the formal reduction potential of RDX. Consequently, the accumulation potential of −0.1 V was selected as an optimum condition for further studies.

Inset Fig. 3 shows the influences of accumulation time on the reduction peak current of 60 μM RDX. The reduction peak current firstly greatly increased with increasing accumulation time, then, after 7.0 min due to adsorption saturation, reaches to steady amount.

3.6. Electrochemical impedance spectroscopy studies

Electrochemical impedance spectroscopy was also employed to investigation of the RDX reduction on the bare GCE and MWCNTs modified electrode. Similar to adsorptive stripping voltammetric experiments, RDX was accumulated at the optimum conditions, pH 7.0, accumulation potential and time −0.1 V and 7.0 min. Fig. 4 shows the bode plots and the Nyquist plots of the impedance (Ω cm^2) and admittance (S cm^2), on the GC (A) and MWCNTs (B) electrodes which were recorded at the dc-offset potential of −0.6 V, 60 μM RDX and pH 7.0. Here, the charge-transfer resistance of the electrode reaction is the only circuit element that has a simple physical meaning describing rate facility of charge transfer during electro-reduction of RDX in the various potentials or analyte concentrations.

The Nyquist diagram of MWCNTs electrode and their related bode and admittance plots on this figure, represent two overlapped, slightly depressed capacitive semicircles. The small semicircle,

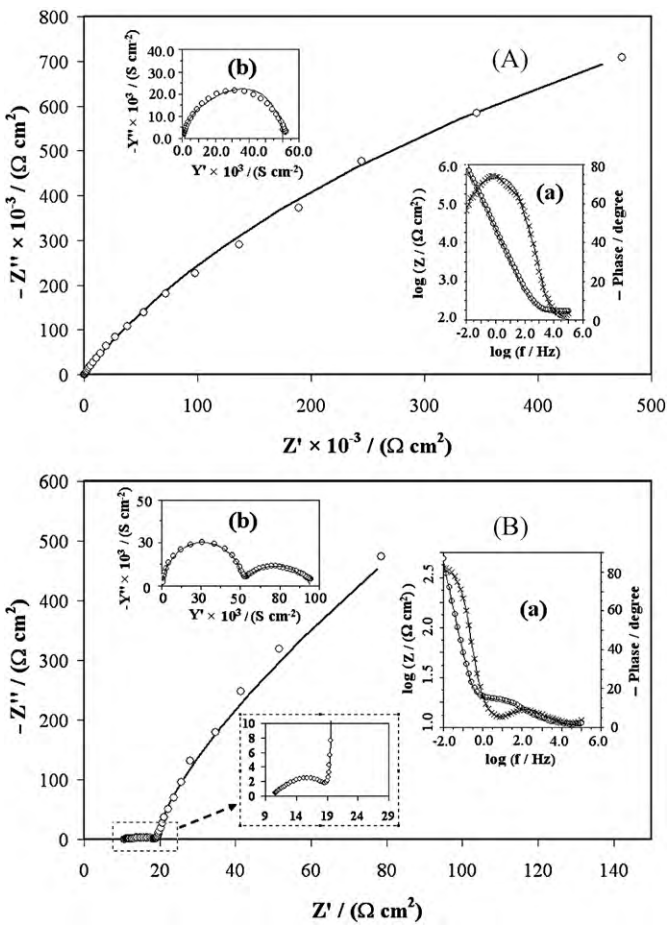

Fig. 4. The Nyquist plots of the impedance (imaginary impedance (Z'') vs. the real impedance (Z')) acquired for 60 μM RDX in pH 7.0 on the GC electrode (A) and MWCNTs electrode (B). Bias in both diagrams was −0.6 V with 5 mV ac voltage amplitude and frequency range of 0.01 Hz to 100 kHz. Insets show their related bode plots (a) and admittance (Y'' vs. Y') plots (b). Points show the experimental data and the full line is calculated from the optimized parameters.

appeared at high-frequencies near the origin, related to the charge-transfer resistance of the first step of RDX reduction (first peak in Fig. 1), with combination of double-layer capacitance. The low-frequencies semicircle can be related to the second step of reduction process, and it has a relatively large diameter (charge-transfer resistance) with respect to the high-frequencies semicircle. This result stems from the fact that the dc-offset potential supplies low over-potential for the second reduction process. The diffusion process observed during the reduction process using the MWCNT electrode most probably appeared at very low-frequencies with a high time constant; it did not appear in the sweeping frequency range in the Nyquist plot. Also, according to the simulated circuits, the GC electrode represents two depressed semicircle with high time constants, demonstrating that the charge transfer resistance of electrochemical reduction process on this electrode is very high [50].

The equivalent circuits compatible with the Nyquist diagrams recorded at the bare GCE and MWCNTs electrodes are depicted in Scheme 1A and B, respectively. The equivalent circuits model consist of solution resistance (R_s), double-layer capacitance (C_{dl}), charge-transfer resistance of the first and second reduction processes ($R_{ct\text{-}1}$ and $R_{ct\text{-}2}$) and their related constant phase elements corresponding to the double-layer capacitances (CPE_1 and CPE_2). The most widely accepted explanation for the presence of constant phase elements and appearance of depressed semicircles in the Nyquist plots is the microscopic roughness which is causing an

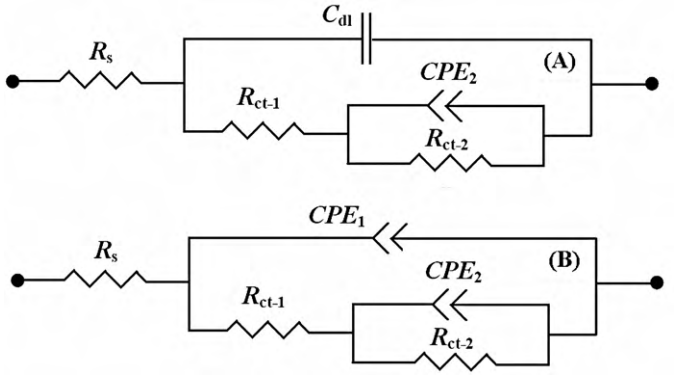

Scheme 1. The equivalent circuits compatible with the Nyquist diagrams represented in Fig. 4.

inhomogeneous distribution in the solution resistance as well as in the double-layer capacitance [51]. Impedance of CPE element can be expressed as [50,52]:

$$Z_{CPE} = Y_0^{-1}(j\omega)^{-n} \quad (3)$$

where Y_0 is admittance parameter ($S\,cm^{-2}\,s^{-n}$) and n represent dimensionless exponent which are independent to frequency; $j = (-1)^{1/2}$ and ω = angular frequency = $2\pi f$. Z_{CPE} corresponds to the constant phase angle element (CPE) impedance. "n" parameter is related to α (phase angle) by $\alpha = (1 - n)\,90^\circ$. So, $n = 1$ and $\alpha = 0$ stand for a perfect capacitor, and lower n values directly reflect the roughness of the electrode surface. When $n = 0.5$, it is equal to a Warburg impedance. When $n = 0$, CPE is reduced to a resistor.

Table 1 shows the values of the equivalent circuit elements obtained by fitting the experimental results. The goodness of the fitting models can be judged by the estimated relative errors presented in the parentheses. According to the values of the electrical equivalent elements reported in this table, upon increasing the concentration of RDX on the MWCNTs electrode, the charge transfer resistances (R_{ct-1} and R_{ct-2}) decreased due to the facile occurrence of the faradic process related to the electro-reduction process. Moreover, the concentration of RDX shows relatively little effect on CPE_1 and CPE_2, related to the double-layer capacitances. The electron transfer resistance R_{ct-1}, for the bare GC and MWCNTs electrode and 60 μM RDX, equals to 361.0 and 9.8 Ω cm^2, respectively, indicating the very faster charge transfer rate for reduction of RDX on the MWCNTs electrode surface, due to the electrocatalytic effect of nanotubes on the electro-reduction process.

3.7. Performance of the system for RDX measurements

The calibration plot of RDX, based on the first reduction peak, shows two linear curves in the concentration region of 0.6–2.0 and 8.0–200.0 μM with detection limit of 25 nM (see Fig. 5). Using adsorptive stripping cyclic voltammetry under the optimum conditions were selected as: pH 7.0 (universal buffer) with a scan rate of 100 mV s^{-1}, and the accumulation time of 7.0 min at potential of −0.1 V, equations of linear least square calibration curves over these ranges are: $I(\mu A) = 57.13\ (\pm 3.68) \times C_{RDX} - 16.20\ (\pm 0.92)$ ($R^2 = 0.9906$) and $I(\mu A) = 2.01\ (\pm 0.080) \times C_{RDX} + 115.81\ (\pm 3.39)$ ($R^2 = 0.9985$), respectively. Relative standard deviation (RSD) of <4% for 60 μM RDX (for 8 analysis) showed excellent reproducibility. No obvious changes in the cathodic peak current were found for the same sample concentration when the modified electrode was kept under ambient conditions for more than 1 month, thus the MWCNTs electrode is stable.

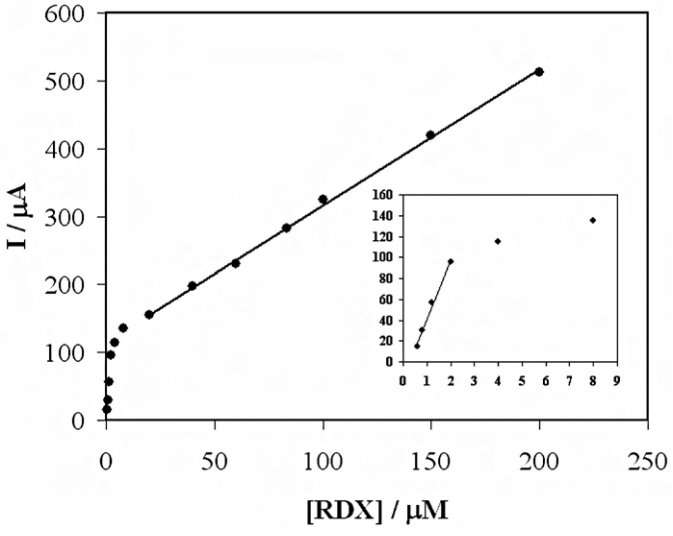

Fig. 5. Calibration curves for the determination of RDX at the optimum conditions. Inset shows the lower concentration range.

This method, as compared to other electrochemical methods [26,27], shows higher sensitivity and lower limit of detection. Also in comparison with the published chromatographic and electrophoresis methods, which require lengthy and tedious extraction procedures, does not require to a significant pretreatment process on the real samples and is rapid, sensitive and simple. Although the chromatographic procedures have the advantage of simultaneous quantitation of the explosives and its related compounds when the chromatographic conditions are properly selected.

3.8. Interference studies

Under optimized experimental conditions described above, the effects of some foreign species on the determination of RDX at 60 μM level were evaluated in detail. The tolerance limit was defined as the maximum concentration of the interfering substance that caused an error less than 3% for determination of RDX. 700-fold of Na^+, K^+, Ca^{2+}, Mg^{2+}, NH_4^+, Cl^-, SO_4^{2-}, CO_3^{2-}, 200-fold of SCN^-, Br^- and I^-, 10-fold of NO_3^- and 2-fold of Fe^{3+} have almost no influence on the current response of RDX. All these indicate that the peak current of RDX is not considerably affected by all conventional

Table 1
The values of the elements in equivalent circuit and the corresponding relative errors for the reduction of RDX on the bare glassy carbon and MWCNTs electrodes.

Electrode	C_{RDX} (μM)	CPE_1		R_{ct-1} (Ω cm^2)	CPE_2		R_{ct-2} (MΩ cm^2)
		$Y_0 \times 10^2$ ($S\,cm^{-2}\,s^n$)	n		$Y_0 \times 10^2$ ($S\,cm^{-2}\,s^n$)	n	
GCE	60.0	1.100 (1.58%)	0.8003 (0.46%)	361.0 (3.21%)	–	–	2.97 (4.23%)
MWCNT	60.0	0.2455 (4.27%)	0.5829 (3.46%)	9.8 (2.92%)	2.803 (1.58%)	0.9978 (0.82%)	1.23 (3.26%)
MWCNT	100.0	0.2653 (4.12%)	0.5755 (3.45%)	9.33 (2.95%)	2.884 (1.62%)	0.9953 (0.84%)	1.19 (1.14%)
MWCNT	200.0	0.2736 (2.77%)	0.5697 (3.13%)	9.25 (2.75%)	2.759 (1.56%)	0.9918 (0.80%)	1.14 (2.87%)
MWCNT	400.0	0.3190 (3.22%)	0.5403 (3.40%)	9.83 (3.18%)	2.622 (1.93%)	0.9769 (0.98%)	1.29 (2.54%)
MWCNT	600.0	0.3684 (2.30%)	0.5175 (2.51%)	10.26 (2.53%)	2.524 (1.61%)	0.9793 (0.82%)	1.35 (3.12%)

Table 2
Determination of RDX in ground water and tap water samples in pH 7.0.

No.	Sample	Added (μM)	Found[a] (μM)	Recovery (%)	RSD (%)
	Ground water				
1		40.00	44.20 ± 4.14	110.5	1.89
2		80.00	73.90 ± 6.33	92.4	2.19
	Tap water				
3		100.00	94.11 ± 9.39	94.1	2.73
4		150.00	136.90 ± 16.87	91.3	3.80

[a] Average of five replicate measurements.

cations, anions and organic substances, but other electrochemically reducible materials such as iron cations can be interfered.

3.9. Application

To evaluate the applicability of the proposed method, the recovery of RDX was determined in the ground water and tap water samples by adding the standard value of RDX to them. Samples were analyzed in accordance with the Section 2.3 and the standard addition method was used for the analysis of prepared samples. The data given in Table 2 show the satisfactory results for analytical determination of RDX in these real samples.

4. Conclusion

The discussed results demonstrated that a electrochemical response of RDX by adsorption stripping voltammetry on the MWCNTs film can remarkably be enhanced in a wide pH range of 2.0–11.0 with a detection limit near to 25 nM at the pH 7.0. This new sensor holds great promise for field-based screening operations, aimed at assisting security surveillance and environmental missions. Such use of nanotube electrodes extends the scope of mentioned method towards widespread important organic compounds that do not show a suitable electrochemical activity at conventional electrodes. Also the reported method can be a useful tool for investigating the interactions of ultratrace level of electroactive organic compounds with MWCNTs. Analysis by this method is comparable to other ultrasensitive techniques and the simplicity, selectivity and short time of process are the main advantages of this procedure, making it useful for routine analysis. This modified electrode can be properly used for determination of RDX in the environmental samples with satisfactory results.

Acknowledgements

The authors wish to thank Isfahan University of Technology (IUT) Research Council and Center of Excellence in Sensor and Green Chemistry and Nano for support of this work.

References

[1] J. Yinon, Field detection and monitoring of explosives, Trends Anal. Chem. 21 (2002) 292–301.
[2] S. Singh, Sensors-an effective approach for the detection of explosives, J. Hazard. Mater. 144 (2007) 15–28.
[3] P.Y. Robidoux, J. Hawari, S. Thiboutot, G. Ampleman, G.I. Sunahara, Chronic toxicity of octahydro-1,3,5,7-tetranitro-1,3,5,7-tetrazocine (HMX) in soil determined using the earthworm (Eisenia andrei) reproduction test, Environ. Pollut. 111 (2001) 283–292.
[4] S.S. Talmage, D.M. Opresko, C.J. Maxwel, C.J.E. Welsh, F.M. Cretella, P.H. Reno, F.B. Daniel, Nitroaromatic munition compounds: environmental effects and screening values, Rev. Environ. Contam. Toxicol. 161 (1999) 1–156.
[5] C.A. Myler, W. Sisk, in: G.S. Sayler, R. Fox, J.W. Blackburn (Eds.), Environmental Biotechnology for Waste Treatment, Plenum Press, New York, NY, 1991, p. 137.
[6] R. Haas, I. Schreiber, E. von Low, G. Stork, Conception for the investigation of contaminated munition plants, Fresenius' J. Anal. Chem. 338 (1990) 41–45.
[7] P.G. Rieger, H.J. Knackmus, in: J.C. Spain (Ed.), Biodegradation of Nitroaromatic Compounds, Plenum Press, New York, 1995, pp. 1–18.
[8] J.E. Walker, D.L. Kaplan, Biological degradation of explosives and chemical agents, Biodegradation 3 (1992) 369–385.
[9] W.D. Won, L.H. DiSalvo, J. Ng, Toxicity and mutagenicity of 2,4,-6-trinitrotoluene and its microbial metabolites, Appl. Environ. Microbiol. 31 (1976) 575–580.
[10] L.E. Winfield, J.H. Rodgers, S.J. D'Surney, The responses of selected terrestrial plants to short (<12 days) and long term (2, 4 and 6 weeks) hexahydro-1,3,5-trinitro-1,3,5-triazine (RDX) exposure. Part I: growth and developmental effects, Ecotoxicology 13 (2004) 335–347.
[11] P.Y. Robidoux, J. Hawari, G. Bardai, L. Paquet, G. Ampleman, S. Thiboutot, G.I. Sudahara, TNT, RDX, and HMX decrease earthworm (Eisenia andrei) life-cycle responses in a spiked natural forest soil, Arch. Environ. Contam. Toxicol. 43 (2002) 379–388.
[12] US EPA, Health Advisory for RDX, US EPA, Washington, DC, 1988.
[13] A. Üzer, E. Erçağ, R. Apak, Spectrophotometric determination of cyclotrimethylenetrinitramine (RDX) in explosive mixtures and residues with the Berthelot reaction, Anal. Chim. Acta 612 (2008) 53–64.
[14] M. Chaloosi, F. Gholamian, M.A. Zarei, Determination of binary mixtures of nitramines by a spectrophotometric method using partial least squares multivariate calibration, Propell. Explos. Pyrotech. 26 (2001) 21–25.
[15] A. Hilmi, J.H.T. Luong, A.L. Nguyen, Development of electrokinetic capillary electrophoresis equipped with amperometric detection for analysis of explosive compounds, Anal. Chem. 71 (1999) 873–878.
[16] C.A. Groom, A. Halasz, L. Paquet, P. D'Cruz, J. Hawari, Cyclodextrin-assisted capillary electrophoresis for determination of the cyclic nitramine explosives RDX, HMX and CL-20: comparison with high-performance liquid chromatography, J. Chromatogr. A 999 (2003) 17–22.
[17] B. Zhang, X. Pan, G.P. Cobb, T.A. Anderson, Use of pressurized liquid extraction (PLE)/gas chromatography–electron capture detection (GC–ECD) for the determination of biodegradation intermediates of hexahydro-1,3,5-trinitro-1,3,5-triazine (RDX) in soils, J. Chromatogr. B 824 (2005) 277–282.
[18] X. Pan, B. Zhang, G.P. Cobb, Extraction and analysis of trace amounts of cyclonite (RDX) and its nitroso-metabolites in animal liver tissue using gas chromatography with electron capture detection (GC–ECD), Talanta 67 (2005) 816–823.
[19] R. Waddell, D.E. Dale, M. Monagle, S.A. Smith, Determination of nitroaromatic and nitramine explosives from a PTFE wipe using thermal desorption-gas chromatography with electron-capture detection, J. Chromatogr. A 1062 (2005) 125–131.
[20] M.E. Walsh, Determination of nitroaromatic, nitramine, and nitrate ester explosives in soil by gas chromatography and an electron capture detector, Talanta 54 (2001) 427–438.
[21] R.L. Marple, W.R. LaCourse, Platform for on-site environmental analysis of explosives using high performance liquid chromatography with UV absorbance and photo-assisted electrochemical detection, Talanta 66 (2005) 581–590.
[22] X. Pan, B. Zhang, S.B. Cox, T.A. Anderson, G.P. Cobb, Determination of N-nitroso derivatives of hexahydro-1,3,5-trinitro-1,3,5-triazine (RDX) in soils by pressurized liquid extraction and liquid chromatography–electrospray ionization mass spectrometry, J. Chromatogr. A 1107 (2006) 2–8.
[23] D.A. Cassada, S.J. Monson, D.D. Snow, R.F. Spalding, Sensitive determination of RDX, nitroso-RDX metabolites, and other munitions in ground water by solid-phase extraction and isotope dilution liquid chromatography–atmospheric pressure chemical ionization mass spectrometry, J. Chromatogr. A 844 (1999) 87–95.
[24] R.L. Marple, W.R. LaCourse, Application of photoassisted electrochemical detection to explosive-containing environmental samples, Anal. Chem. 77 (2005) 6709–6714.
[25] T. Khayamian, M. Tabrizchi, M.T. Jafari, Analysis of 2,4,6-trinitrotoluene, pentaerythritol tetranitrate and cyclo-1,3,5-trimethylene-2,4,6-trinitramine using negative corona discharge ion mobility spectrometry, Talanta 59 (2003) 327–333.
[26] S.Y. Ly, D.H. Kim, M.H. Kim, Square-wave cathodic stripping voltammetric analysis of RDX using mercury-film plated glassy carbon electrode, Talanta 58 (2002) 919–926.
[27] N. Pon Saravanan, S. Venugopalan, N. Senthilkumar, P. Santhosh, B. Kavita, H. Gurumallesh Prabu, Voltammetric determination of nitroaromatic and nitramine explosives contamination in soil, Talanta 69 (2006) 656–662.
[28] H.X. Zhang, A.M. Cao, J.S. Hu, L.J. Wan, S.T. Lee, Electrochemical sensor for detecting ultratrace nitroaromatic compounds using mesoporous SiO_2-modified electrode, Anal. Chem. 78 (2006) 1967–1971.
[29] J. Wang, R. Polsky, B. Tian, M.P. Chatrathi, Voltammetry on microfluidic chip platforms, Anal. Chem. 72 (2000) 5285–5289.
[30] R.G. Bozic, A.C. West, R. Levicky, Square wave voltammetric detection of 2,4,6-trinitrotoluene and 2,4-dinitrotoluene on a gold electrode modified with self-assembled monolayers, Sens. Actuators B 133 (2008) 509–515.
[31] J. Wang, G. Liu, H. Wu, Y. Lin, Sensitive electrochemical immunoassay for 2,4,6-trinitrotoluene based on functionalized silica nanoparticle labels, Anal. Chim. Acta 610 (2008) 112–118.
[32] Y. Zimmermann, J.A.C. Broekaert, Determination of TNT and its metabolites in water samples by voltammetric techniques, Anal. Bioanal. Chem. 383 (2005) 998–1002.
[33] L. Agüí, D. Vega-Montenegro, P. Yáñez-Sedeño, J.M. Pingarrón, Rapid voltammetric determination of nitroaromatic explosives at electrochemically activated carbon-fibre electrodes, Anal. Bioanal. Chem. 382 (2005) 381–387.

[34] J. Wang, F. Lu, D. MacDonald, J. Lu, M.E.S. Ozsoz, K.R. Rogers, Screen-printed voltammetric sensor for TNT, Talanta 46 (1998) 1405–1412.
[35] J. Wang, S.B. Hocevar, B. Ogorevc, Carbon nanotube-modified glassy carbon electrode for adsorptive stripping voltammetric detection of ultratrace levels of 2,4,6-trinitrotoluene, Electrochem. Commun. 6 (2004) 176–179.
[36] J. Wang, S. Thongngamdee, D. Lu, Sensitive voltammetric sensing of the 2,3-dimethyl-2,3-dinitrobutane (Dmnb) explosive taggant, Electroanalysis 18 (2006) 971–975.
[37] R. Sivabalan, M.B. Talawar, P. Santhosh, N. Senthilkumar, B. Kavitha, G.M. Gore, S. Venugopalan, Electro-analysis of energetic materials, J. Hazard. Mater. 148 (2007) 573–582.
[38] J. Wang, Electrochemical sensing of explosives, Electroanalysis 19 (2007) 415–423.
[39] A. Salimi, R. Hallaj, G.R. Khayatian, Amperometric detection of morphine at preheated glassy carbon electrode modified with multiwall carbon nanotubes, Electroanalysis 17 (2005) 873–879.
[40] J. Wang, G. Chen, M.P. Chatrathi, M. Musameh, Capillary electrophoresis microchip with a carbon nanotube-modified electrochemical detector, Anal. Chem. 76 (2004) 298–302.
[41] B. Rezaei, S. Damiri, Multiwalled carbon nanotubes modified electrode as a sensor for adsorptive stripping voltammetric determination of hydrochlorothiazide, IEEE Sens. J. 8 (2008) 1523–1529.
[42] A. Merkoçi, M. Pumera, X. Llopis, B. Pérez, M. del Valle, S. Alegret, New materials for electrochemical sensing VI: carbon nanotubes, Trends Anal. Chem. 24 (2005) 826–838.
[43] J.J. Gooding, Nanostructuring electrodes with carbon nanotubes: a review on electrochemistry and applications for sensing, Electrochim. Acta 50 (2005) 3049–3060.
[44] C.E. Banks, R.G. Compton, New electrodes for old: from carbon nanotubes to edge plane pyrolytic graphite, Analyst 131 (2006) 15–21.
[45] A.F. Holloway, G.G. Wildgoose, R.G. Compton, L. Shao, M.L.H. Green, The influence of edge-plane defects and oxygen-containing surface groups on the voltammetry of acid-treated, annealed and "super-annealed" multi-walled carbon nanotubes, J. Solid State Electrochem. 12 (2008) 1337–1348.
[46] C.E. Banks, R.R. Moore, T.J. Davies, R.G. Compton, Investigation of modified basal plane pyrolytic graphite electrodes: definitive evidence for the electrocatalytic properties of the ends of carbon nanotubes, Chem. Commun. 16 (2004) 1804–1805.
[47] H.M. Heilmann, U. Wiesmann, M.K. Stenstrom, Kinetics of the alkaline hydrolysis of high explosives RDX and HMX in aqueous solution and adsorbed to activated carbon, Environ. Sci. Technol. 30 (1996) 1485–1492.
[48] S. Hwang, D.R. Felt, E.J. Bouwer, M.C. Brooks, S.L. Larson, J.L. Davis, Remediation of RDX-contaminated water using alkaline hydrolysis, J. Environ. Eng. 132 (2006) 256–262.
[49] A.J. Bard, L.R. Faulkner, Electrochemical Methods: Fundamentals and Applications, 2nd ed., John Wiley and Sons, New York, 2001, pp. 231–236.
[50] E. Barsoukov, J.R. Macdonald, Impedance Spectroscopy: Theory, Experiment, and Applications, 2nd ed., Wiley, New Jersey, 2005.
[51] A. Maritan, F. Toigo, On skewed arc plots of impedance of electrodes with an irreversible electrode process, Electrochim. Acta 35 (1990) 141–145.
[52] User Manual for Software FRA 4.9, Autolab System, Eco Chemie B.V., The Netherlands, 2007.